JACS
JOURNAL OF THE AMERICAN CHEMICAL SOCIETY
Article
pubs.acs.org/JACS

Difference in Energy between Two Distinct Types of Chalcogen Bonds Drives Regioisomerization of Binuclear (Diaminocarbene)Pd^{II} Complexes

Alexander S. Mikherdov, Mikhail A. Kinzhalov, Alexander S. Novikov, Vadim P. Boyarskiy,* Irina A. Boyarskaya, Dmitry V. Dar'in, Galina L. Starova, and Vadim Yu. Kukushkin*

Saint Petersburg State University, 7/9 Universitetskaya Nab., Saint Petersburg, 199034, Russian Federation

Supporting Information

ABSTRACT: The reaction of *cis*-[$PdCl_2(CNXyl)_2$] (Xyl = 2,6-$Me_2C_6H_3$) with various 1,3-thiazol- and 1,3,4-thiadiazol-2-amines in chloroform gives a mixture of two regioisomeric binuclear diaminocarbene complexes. For 1,3-thiazol-2-amines the isomeric ratio depends on the reaction conditions and *kinetically* (**KRs**) or *thermodynamically* (**TRs**) *controlled regioisomers* were obtained at room temperature and on heating, respectively. In $CHCl_3$ solutions, the isomers are subject to reversible isomerization accompanied by the cleavage of Pd−N and C−N bonds in the carbene fragment XylNCN(R)Xyl. Results of DFT calculations followed by the topological analysis of the electron density distribution within the formalism of Bader's theory (AIM method) reveal that in $CHCl_3$ solution the relative stability of the regioisomers (ΔG_{exp} = 1.2 kcal/mol; ΔG_{calcd} = 3.2 kcal/mol) is determined by the energy difference between two types of the intramolecular chalcogen bonds, viz. S···Cl in **KRs** (2.8−3.0 kcal/mol) and S···N in **TRs** (4.6−5.3 kcal/mol). In the case of the 1,3,4-thiadiazol-2-amines, the regioisomers are formed in approximately equal amounts and, accordingly, the energy difference between these species is only 0.1 kcal/mol in terms of ΔG_{exp} (ΔG_{calcd} = 2.1 kcal/mol). The regioisomers were characterized by elemental analyses (C, H, N), HRESI$^+$-MS and FTIR, 1D (^{1}H, ^{13}C{^{1}H}) and 2D (^{1}H,^{1}H-COSY, ^{1}H,^{1}H-NOESY, ^{1}H,^{13}C-HSQC, ^{1}H,^{13}C-HMBC) NMR spectroscopies, and structures of six complexes (three **KRs** and three **TRs**) were elucidated by single-crystal X-ray diffraction.

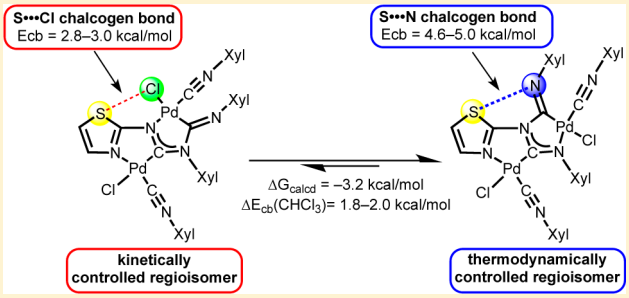

INTRODUCTION

Chalcogen bonding (CB) is usually defined as noncovalent interaction between a localized positive region on a chalcogen atom in the extension of the covalent bonds (σ-hole) and electron donor species serving as CB acceptors.[1] The phenomenon of CB currently attracts great attention due to applicability of CB in biochemistry,[2] drug design,[2d,3] polymer science,[4] crystal engineering,[5] and supramolecular chemistry.[6] Although heavier chalcogens, Se[7] and Te,[6f,8] are better CB donors because of their higher polarizability,[1b−d] the majority of recent reports deal with CBs involving more abundant S centers. Most common types of CB with S atoms are S···S, S···O, and S···N interactions that are widely available in proteins[2a−c] and also in some organic compounds.[6b,e,g,9] The CBs of sulfur with halogens (particularly with Cl centers in both organic species[10] and metal complexes[11]) are also known, albeit still unusual.

The ability of CB to control the structures of *S*-containing compounds (e.g., conformational stabilization),[3c,f,12] their molecular assembly,[6] protein folding,[2a−c,13] and molecular recognition[2e] was repeatedly reported, whereas *the effect of CB on reactivity* was exceptionally rarely verified. The dominant part of the published examples deals with stabilization through CB of certain conformation either in starting compounds or in intermediates. These works include the application of the chiral isothiourea derivatives as organocatalysts that act via formation of intramolecular S···O CB in the intermediate,[14] stabilization of an intermediate in Pummerer reaction by inter- and intramolecular S···O contacts,[15] facilitation of the intramolecular redox cyclization of S-containing diazene,[16] the photocyclization of 2,3-dithiazolylbenzothiophene,[17] and the bond-switch rearrangement of substituted isothiadiazoles and isothiazoles[18] by formation in both cases intramolecular S···N CBs in the starting compounds. The other reports disclose electronic effects of CB on the reaction center, viz. facilitation of the S−S bond cleavage in benzo-1,2-dithiolan-3-one-1-oxides by formation of either S···O, or S···Cl contacts,[19] the protodeboronation of 5-thiazolyl boronic acid[20] and the Mann−Pope reaction[21] which are driven by intramolecular S···O interactions. Thus, only one example when the reactivity is affected by S···Cl CB is known.

In this work, we continued our project focused on the ligand reactivity of acyclic diaminocarbenes giving, after the coupling

Received: August 31, 2016
Published: October 4, 2016

DOI: 10.1021/jacs.6b09133
J. Am. Chem. Soc. 2016, 138, 14129−14137

with the isocyanide species, the binuclear palladium(II) complexes.[22] When 1,3-thiazol- and 1,3,4-thiadiazol-2-amines were applied as reactivity partners, we have now found that the reaction of *cis*-[$PdCl_2(CNXyl)_2$] (Xyl = 2,6-$Me_2C_6H_3$) and these heterocycles leads to a mixture of two regioisomeric binuclear diaminocarbene species. In the case of 1,3-thiazol-2-amines, the two structures are held by intramolecular S···Cl (for kinetically controlled isomers) or S···N (for thermodynamically controlled isomers) CBs and the energy difference between these noncovalent interactions drives the regioisomerization. The most relevant example is the reversible bond-switch rearrangement of substituted isothiadiazoles and isothiazoles,[18b,c] where the products and the starting compounds are involved in the identical S···N interactions; these CBs led to stabilization of the *syn*-conformation required for occurrence of the reaction.

To the best of our knowledge, this work is the first example of a system where the chemical reactivity (regioisomerization) mainly depends on the energy difference between two distinctive types of CB, viz. S···Cl and S···N.

RESULTS AND DISCUSSION

Generation of Binuclear Aminocarbenes. The treatment of the palladium(II) complex *cis*-[$PdCl_2(CNXyl)_2$] (**PC**) with 1,3-thiazol-2-amines (**1**−**6**; Figure 1) in a molar ratio 1:1.5

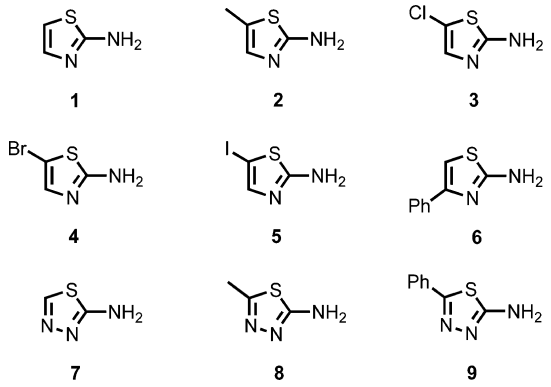

Figure 1. Heterocycles employed for the reactivity study.

in $CDCl_3$ at RT in each case gives a mixture of two binuclear aminocarbene products (Scheme 1) corresponding to *kinetically* (**KR1**−**6**) and *thermodynamically* (**TR1**−**6**) *controlled regioisomers* formed in (3−7):1 ratios depending on the nature of the 1,3-thiazoles (Table S1, Supporting Information).

Scheme 1. Reaction between PC and 1−9

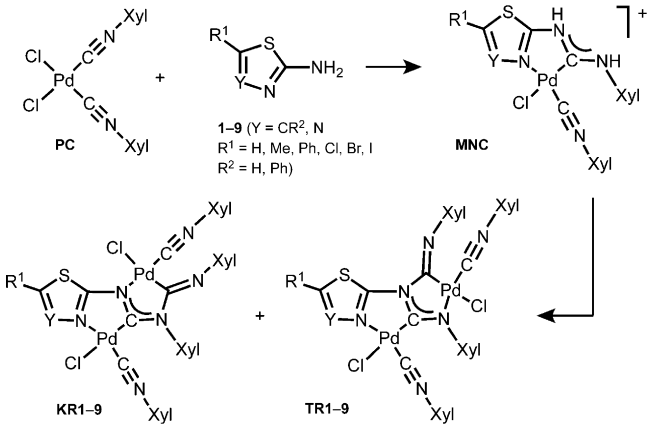

When this reaction was conducted upon reflux, an isomeric ratio **KR**/**TR1**−**6** was 1:(3−7) thus indicating predominant generation of thermodynamically controlled product (Table S1).

The isomeric ratio is different in the reaction of **PC** with 1,3,4-thiadiazol-2-amines (**7**−**9**; Figure 1). At room temperature an isomeric ratio was (2−3):1 for **KR**/**TR7**−**8**, whereas upon reflux it was ca. 13:10 for **KR**/**TR7** and ca. 10:11 for **KR**/**TR8**. In the reaction with **9**, isomeric ratio **KR**/**TR9** is almost independent of the synthesis temperature, viz. ca. 11:9 at RT and ca. 10:11 upon reflux (Table S1).

Kinetically controlled complexes **KR1**−**5** and **KR7**−**9** were isolated from the reaction mixtures that were obtained at RT, whereas **TR1**−**4**, **TR6**, **TR8**, and **TR9** were isolated from the mixtures formed upon reflux (Table S1). Procedure of isolation of pure **TR5** is different due to instability of **5** under reflux conditions (the **KR**/**TR5** yield was only 30%) and **TR5** was isolated from the equilibrium mixture obtained at 45 °C (Table 1). In all cases, the appropriate mixtures were evaporated to dryness in air and then the residue was redissolved in a CH_2Cl_2−Me_2CO system and the solution was subjected to fractional crystallization on slow evaporation. All our attempts to isolate isomerically pure **KR6** and **TR7** failed and each of these species were obtained only in a mixture with the other regioisomer.

We believe that the generation of isomers **KR** and **TR** proceeds by deprotonation of the initially formed mononuclear aminocarbene complex (**MNC**; Scheme 1) followed by its coupling with a XylNC in **PC**. The deprotonation increases the nucleophilic activity of the NCN group and, subsequently, provides its addition to two electrophilic centers (at a ligated isocyanide carbon and at the metal center) of another molecule of the starting palladium(II) isocyanide complex as we suggested earlier for the adduct with pyridin-2-amine.[22] In this work, **MNCs** were not obtained directly even on slow addition of a suspension of **PC** in $CDCl_3$ to 3- or 4-fold molar excess of any one of **1**−**9** in $CDCl_3$ at either RT, or upon reflux. This could be due to the electron withdrawing character of the 1,3-thiazole and 1,3,4-thiadiazole rings (e.g., pK_a 5.32 for 1,3-thiazol-2-amine[23] vs 6.71 for pyridin-2-amine[24]), which facilitates the deprotonation of **MNC**. By contrast, the reaction with pyridin-2-amine requires the presence of a base.[22] The appearance of **MNC** and its deprotonated form in the reaction between **PC** and **1** was confirmed by HRESI$^+$-MS (calcd for $C_{21}H_{22}ClN_4PdS^+$ 503.0284, found *m*/*z* 503.0280 [M − Cl]$^+$ and calcd for $C_{21}H_{21}N_4PdS^+$ 467.0517, found *m*/*z* 467.0520 [M − Cl − HCl]$^+$).

Characterization of the Regioisomers. All solid isomeric mixtures gave satisfactory microanalyses (C, H, N). Pure complexes were obtained as yellow solids and characterized by high resolution ESI$^+$-MS, FTIR, 1D (^{1}H, ^{13}C{^{1}H}) and 2D (^{1}H,^{1}H-COSY, ^{1}H,^{1}H-NOESY, ^{1}H,^{13}C-HSQC, ^{1}H,^{13}C-HMBC) NMR spectroscopies (Supporting Information). Complexes **KR6** and **TR7** were characterized only by ^{1}H NMR spectroscopy in the isomeric mixtures (see above). In addition, the solid state structures of **KR1**, **KR7**, **KR9**, **TR1**, **TR7**, and **TR8** were elucidated by single-crystal X-ray diffraction.

For all complexes the HRESI$^+$ mass spectra display a fragmentation pattern corresponding to [M − Cl]$^+$ with the characteristic isotopic distribution. The FTIR spectra for **KRs** and **TRs** exhibit one or two strong and broad ν(C≡N) bands

DOI: 10.1021/jacs.6b09133
J. Am. Chem. Soc. 2016, 138, 14129−14137

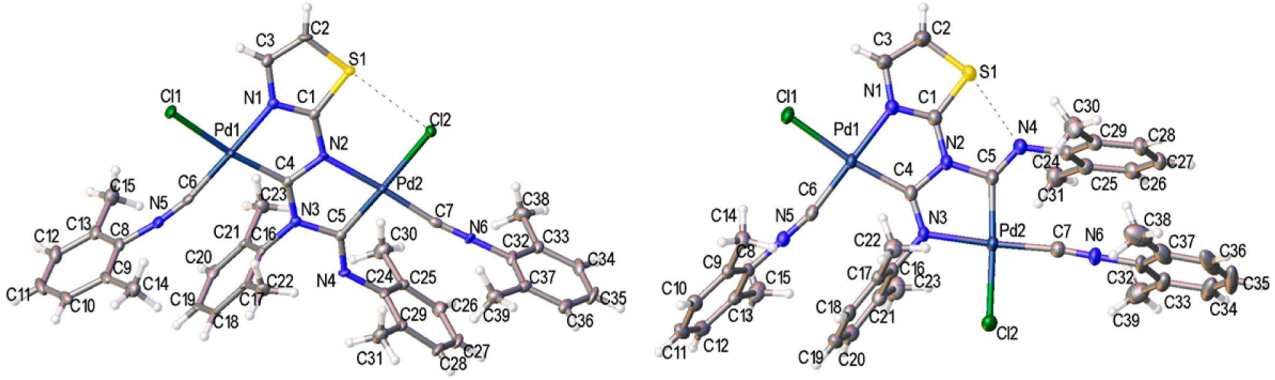

Figure 2. Views of **KR1** (left) and **TR1** (right) with the atomic numbering scheme. Thermal ellipsoids are drawn at the 50% probability level. Dotted lines indicate the S···Cl and S···N contacts. Selected bond distances (Å) and angles (deg) for **KR1**: Pd1−C4 2.024(6), N2−C4 1.365(8), N3−C4 1.312(9), Pd2−C5 1.991(6), N3−C5 1.451(9), N4−C5 1.260(9), N5−C6 1.155(9), N6−C7 1.149(9), S1−Cl2 3.097(2), C2−S1−Cl2 172.0(3). Selected bond distances (Å) and angles (deg) for **TR1**: Pd1−C4 2.018(3), N2−C4 1.407(5), N3−C4 1.280(5), Pd2−C5 1.990(4), N2−C5 1.427(4), N4−C5 1.267(5), N5−C6 1.152(4), N6−C7 1.144(5), S1−N4 2.672(3), C2−S1−N4 160.65(16).

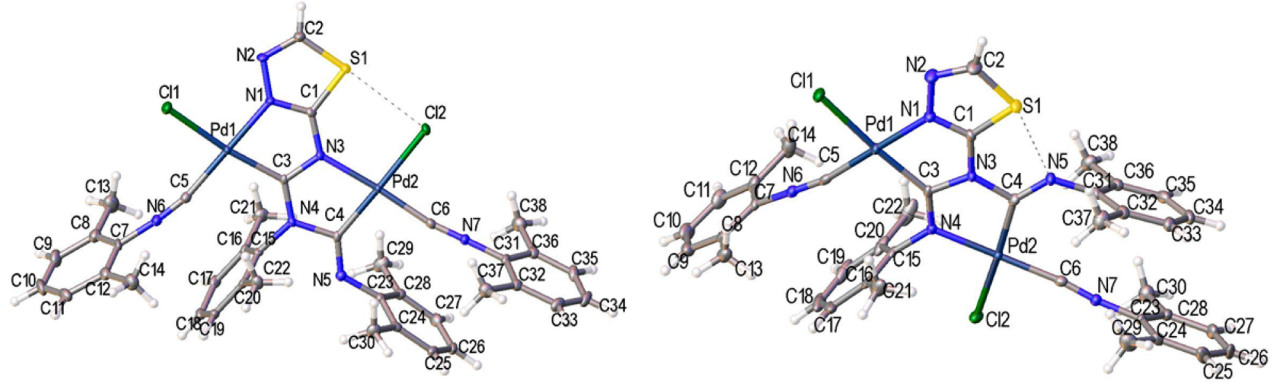

Figure 3. Views of **KR7** (left) and **TR7** (right) with the atomic numbering scheme. Thermal ellipsoids are drawn at the 50% probability level. Dotted lines indicate the S···Cl and S···N contacts. Selected bond distances (Å) and angles (deg) for **KR7**: Pd1−C3 2.016(2), N3−C3 1.363(3), N4−C3 1.328(3), Pd2−C4 1.985(2), N4−C4 1.471(3), N5−C4 1.258(3), N6−C5 1.145(4), N7−C6 1.152(4), S1−Cl2 3.0927(9), Cl2−S1−C2 172.79(12). Selected bond distances (Å) and angles (deg) for **TR7**: Pd1−C3 2.016(2), N3−C3 1.412(4), N4−C3 1.285(4), Pd2−C4 1.955(3), N3−C4 1.477(4), N5−C4 1.268(4), N6−C5 1.151(4), N7−C6 1.148(4), S1−N5 2.702(3), C2−S1−N5 157.45(13).

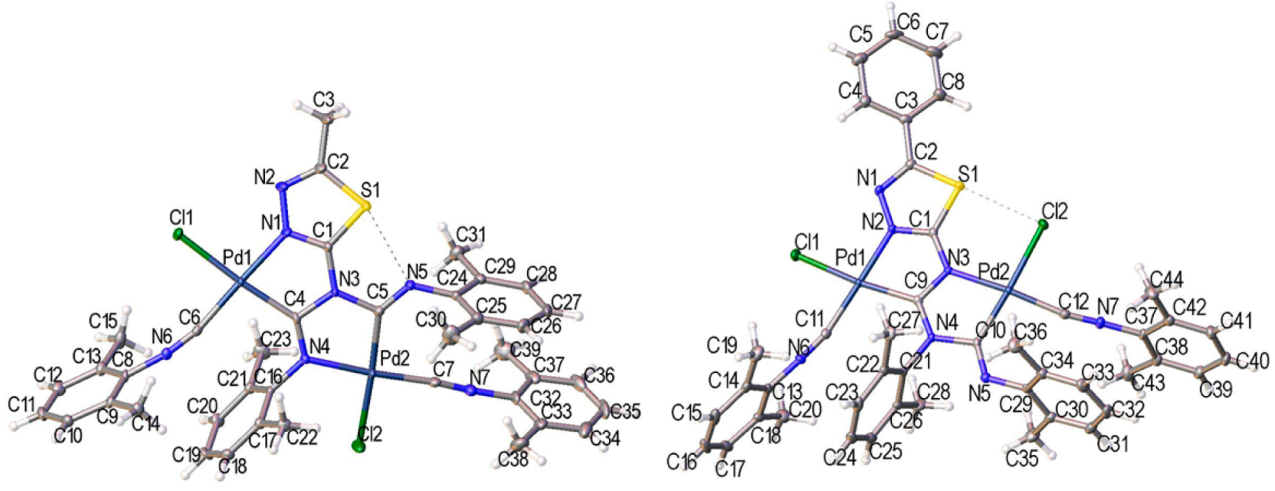

Figure 4. Views of **TR8** (left) and **KR9** (right) with the atomic numbering scheme. Thermal ellipsoids are drawn at the 50% probability level. Dotted lines indicate the S···Cl and S···N contacts. Selected bond distances (Å) and angles (deg) for **TR8**: Pd1−C4 2.003(4), N4−C4 1.288(5), N3−C4 1.415(5), N3−C5 1.444(6), N5−C5 1.258(5), Pd2−C5 1.995(4), N6−C6 1.145(5), N7−C7 1.155(6), S1−N5 2.740(4), C2−S1−N5 156.89(17). Selected bond distances (Å) and angles (deg) for **KR9**: Pd1−C9 2.009(3), N4−C9 1.331(4), N3−C9 1.357(4), N4−C10 1.465(4), N5−C10 1.259(4), Pd2−C10 1.985(3), C11−N6 1.149(4), C12−N7 1.145(4), S1−Cl2 3.0511(10), C2−S1−Cl2 177.90(11).

DOI: 10.1021/jacs.6b09133
J. Am. Chem. Soc. 2016, 138, 14129−14137

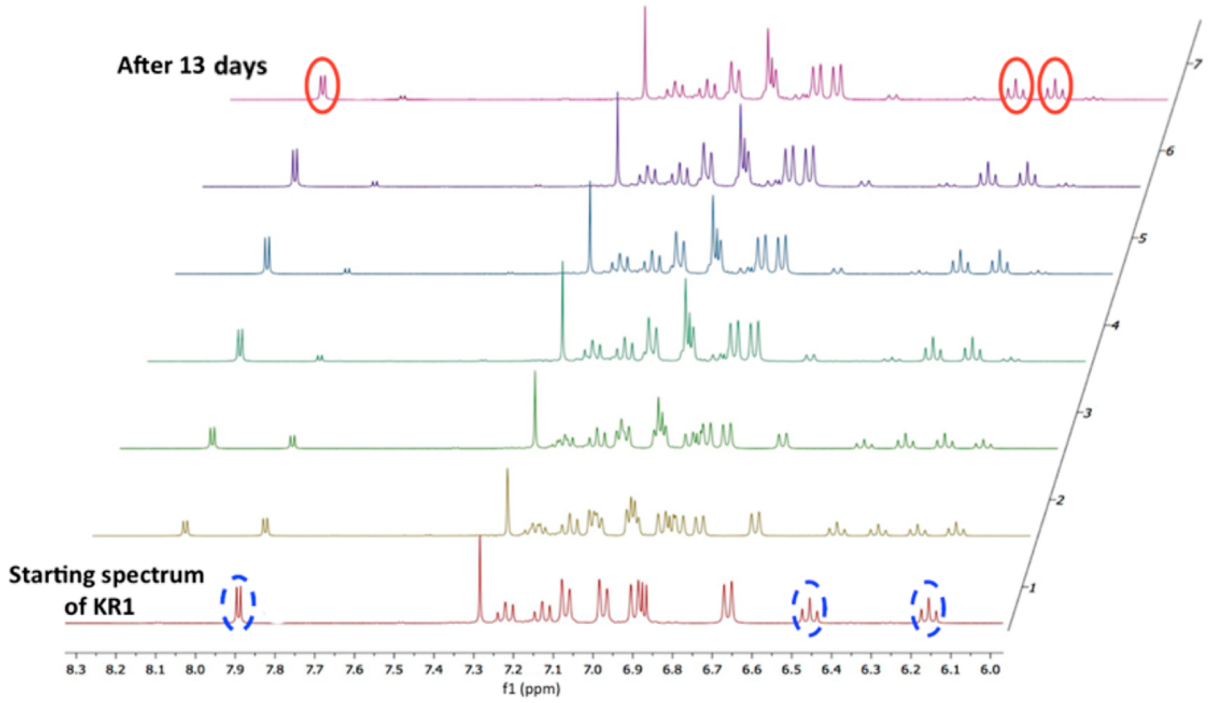

Figure 5. ^{1}H NMR monitoring of isomerization **KR1** into **TR1** in $CDCl_3$ at 45 °C.

in the range 2215−2190 cm^{-1} from both RNC ligands in each species. In addition, **KRs** demonstrate three ν(C═N) strong bands near 1635, 1470, and 1430 cm^{-1} in contrast to three ν(C═N) bands at ca. 1620, 1550, and 1470 cm^{-1} observed for **TRs**.

The ^{1}H NMR spectra of **KRs** and **TRs** display a set of overlapped and individual signals in the δ 7.25−6.05 range assigned to the 12 aromatic C−H protons in the *meta*- and *para*-positions of the xylyl groups and the individual group of signals of the thiaazaheterocyclic fragment in the δ 8.65−6.75 range. Signals of the Me groups were observed in δ 2.50−2.00 interval as four resolved singlets for **KRs** and as two resolved and two overlapped singlets for **TRs**.

The ^{13}C{^{1}H} NMR spectra of all **KRs** and **TRs** exhibit two signals of carbons in the NCN fragments near δ 195 and 165 for **KRs** and near δ 180 and 160 for **TRs**. These resonances belong to the range specific for Pd−$C_{carbene}$ (δ_C 160−224) in acyclic diaminocarbenes.[22,25] Remarkable that the NCN carbon signals of **KRs** and **TRs** are different. The assignments of the ^{1}H and ^{13}C signals were performed by ^{1}H,^{1}H-COSY, ^{1}H,^{1}H-NOESY, ^{1}H,^{13}C-HSQC, ^{1}H,^{13}C-HMBC NMR methods (see Supporting Information).

The crystal data, data collection parameters, and structure refinement data of **KR1**, **KR7**, **KR9**, **TR1**, **TR7**, and **TR8** are given in Table S2 (Supporting Information). The plots of the structures with selected bond lengths and angles are given in Figures 2−4.

Generally, the molecules lie in one slightly distorted plane with an exception of the xylyl groups. In **KRs** and **TRs**, both metal centers adopt a distorted square planar geometry. The isocyanide ligands are in the *cis*-position to the NCN fragments. In each complex, the bond lengths of the two coordinated CN groups fall in the interval of 1.144−1.155 Å that is typical for the common range of the CN triple bonds in the related isocyanide palladium complexes, e.g., [$PdX_2(CNXyl)_2$] (1.145−1.156 Å; X = Cl,[26] Br[27]).

The structure of **KRs** is similar to that for the relevant binuclear aminocarbene complexes also bearing four adjacent xylyl substituents.[22] In the metallacycles of **KRs**, the angles around the palladium(II) centers are within the 78.25(9)−80.78(11)° range being slightly larger to those previously observed in the similar pyridin-2-amine based binuclear aminocarbene complex [78.73(9)−79.36(8)°].[22] In **TRs**, these angles are larger than in **KRs** (79.93−81.70°). The Pd−C distances (**KR1**: Pd1−C4 2.024(6), Pd2−C5 1.991(6); **KR7**: Pd1−C3 2.016(2), Pd2−C4 1.985(2); **KR9**: Pd1−C9 2.009(3), Pd2−C10 1.985(3); **TR1** Pd1−C4 2.018(3), Pd2−C5 1.990(3); **TR7**: Pd1−C3 2.016(2), Pd2−C4 1.955(3); **TR8**: Pd1−C4 2.003(4), Pd2−C5 1.995(4) Å) are longer than those reported for the previously observed for the pyridin-2-amine based binuclear aminocarbene complex (1.988(2) and 1.977(2) Å).[22]

In **KRs**, the lengths of the C−N bonds in the NCN fragment connected to Pd1 are close (**KR1**: C4−N3 1.312(9), C4−N2 1.365(9); **KR7**: C3−N3 1.363(3), C3−N4 1.328(3); **KR9**: C9−N3 1.357(4) Å, C9−N4 1.331(4) Å) and they are intermediate between the typical double and single bonds reflecting the diaminocarbene nature. In the other NCN fragment connected to Pd2, one bond (**KR1**: N3−C5 1.451(9); **KR9**: N4−C4 1.471(3); **KR6**: N4−C10 1.465(4) Å) is a single bond (1.452(8) Å),[28] while the other bond (**KR1**: N4−C5 1.260(9); **KR7**: N5−C4 1.258(3); **KR9**: N5−C10 1.259(4) Å) is a typical double bond (1.260(9) Å).[28] In **TRs**, one C−N bond in each NCN fragment is single (**TR1**: C4−N2 1.407(4), C5−N2 1.427(4); **TR7**: N3−C3 1.412(4), N3−C4 1.477(4); **TR8**: N3−C4 1.415(5), N3−C5 1.444(6) Å) and another one is closer to the double bond (**TR1**: C4−N3 1.280(5), C5−N4 1.2677(5); **TR7**: N4−C3 1.285(4), N5−C4 1.268(4); **TR8**: N4−C4 1.288(5), N5−C5 1.258(5) Å).

X-ray diffraction data also indicate that the S···Cl (**KR1**: S1···Cl2 3.097(2); **KR7**: S1···Cl2 3.0927(9); **KR9**: S1···Cl2 3.0511(10) Å) distances in **KRs** and S···N (**TR1**: S1···N4

DOI: 10.1021/jacs.6b09133
J. Am. Chem. Soc. 2016, 138, 14129−14137

2.672(3); **TR7**: S1···N5 2.702(3); **TR8**: S1···N5 2.740(4) Å) in **TRs** are less than the sum of Rowland's van der Waals radii[29] of these atoms (vdw r(S + Cl) = 3.57, vdw r(S + N) = 3.45 Å and even Bondi's[30] vdw separations (r(S + Cl) = 3.55, r(S + N) = 3.35 Å)) and the angles C2−S1−X (X = Cl for **KRs** or N for **TRs**) are within the 156.89(17)−177.90(11)° range and this suggests the presence of chalcogen bonding[1d,e,31] between the S and Cl centers in **KRs** and between the S and N atoms in **TRs**. Both the S···Cl and S···N contacts are among short CBs reported (the shortest S···Cl is 2.982 Å[10a] and S···N is 2.324 Å[32]).

All other bond lengths in **KRs** and **TRs** are typical, and their values agree with those reported for related palladium(II) carbene and isocyanide complexes.[26,33]

The Regioisomerization. The isomerization of **KR1** into **TR1** at 45 °C was monitored by IR spectroscopy in $CHCl_3$ and by NMR in $CDCl_3$ (Figure 5). In the IR spectra, each isomer has a specific band used for monitoring, viz. 1431 cm^{-1} (**KR1**) that losses its intensity upon isomerization and 1556 cm^{-1} (**TR1**) that increasing in time; two isosbestic points at 1458 cm^{-1} and at 1349 cm^{-1} were observed indicating the presence of two interconvertible forms. However, insofar as the isomerization is very slow, monitoring by NMR is much simpler and we used this method to achieve and to characterize the equilibrium.

When pure isomers **KR1** and **TR1** were dissolved in $CDCl_3$ and both solutions were kept at RT, in their NMR spectra we observed appearance of signals of the other isomer. The isomerization is slow and at 45 °C the equilibrium (1:7, respectively; obtained by ^{1}H NMR integration; Figure 5: blue ovals indicate selected signals of **KR1**, whereas red ovals, selected signals of **TR1**) was reached after 13 days.

The isomerization of other complexes was also studied by NMR in $CDCl_3$ at 45 °C (Table 1). For all studied complexes

Table 1. Equilibrium Ratios and Constants Based on ^{1}H NMR Monitoring at 45 °C

mixture	equilibrium ratios	equilibrium constant
KR/TR1	13:87	6.7
KR/TR2	17:83	4.9
KR/TR3	15:85	5.7
KR/TR4	14:86	6.1
KR/TR5	15:85	5.7
KR/TR6	14:86	6.1
KR/TR7	46:54	1.2
KR/TR8	48:52	1.1
KR/TR9	45:55	1.2

with **7**−**9** (**KR/TR7**−**9**) the equilibrium ratio between **KRs** and **TRs** is close 9:11 compared to 1:(5−7) for the studied 1,3-thiazol-2-amines adducts (**KR/TR1**−**6**). As can be inferred from the obtained data, the substitution in a heterocycle does not significantly affect the equilibrium ratio, whereas the addition of one more nitrogen atom in the heterocycle lead to substantial change of relative stability of the regioisomers.

The observed regioisomerization cannot proceed without splitting the Pd−N and C−N bonds of the aminocarbene fragment.

The only known reversible formation of palladium diaminocarbene backbone in a solution was reported by Slaughter and co-workers for *intramolecular* chelate ring opening in a palladium(II) *bis*-carbene complex (Scheme 2).[34] To the best of our knowledge, we found the first example of the *intermolecular* regioisomerization of palladium amino-

Scheme 2. Reversible Ring Opening[34]

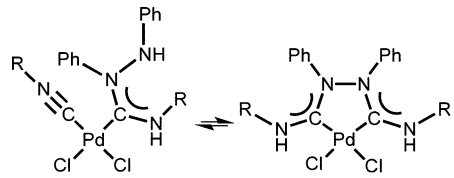

carbene complexes accompanied by the splitting of the C−N bond in the carbene fragment.

Theoretical Consideration of the Effect of CB on the Isomerization. Inspection of the crystallographic data suggests the presence of the chalcogen bonds S···Cl and S···N in all **KRs** and **TRs**. In order to confirm or deny the hypothesis on the existence of these noncovalent interactions and to estimate the contribution of these weak interactions to the stabilization of regioisomers in a $CHCl_3$ solution, we carried out DFT calculations and performed topological analysis of the electron density distribution within the formalism of Bader's theory (AIM method)[35] for two isomeric pairs of the simplest studied 1,3-thiazole- (**KR/TR1**) and 1,3,4-thiadiazole- (**KR/TR7**) derived complexes. We successfully used this approach upon studies of noncovalent interactions and properties of coordination bonds in transition metal complexes.[11b,36] The results are summarized in Table S3 (Supporting Information), the contour line diagrams of the Laplacian distribution $\nabla^2\rho(\mathbf{r})$, bond paths, and selected zero-flux surfaces for **KR1** and **TR1** are shown in Figure 6. The Poincare−Hopf relationship in all cases is satisfied; thus, all critical points have been found.

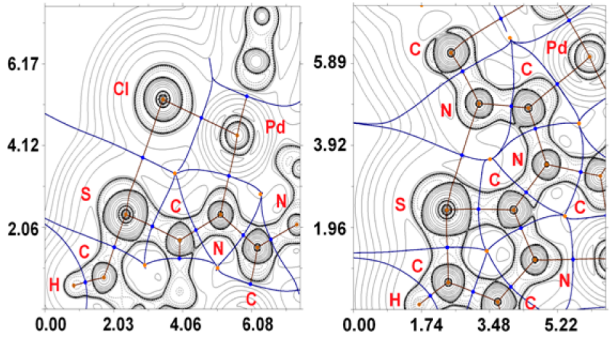

Figure 6. Contour line diagrams of the Laplacian distribution $\nabla^2\rho(\mathbf{r})$, bond paths and selected zero-flux surfaces for **KR1** (left) and **TR1** (right) in solid state. Bond critical points (3, −1) are shown in blue; nuclear critical points (3, −3), in pale brown; ring critical points (3, +1), in orange; length unit, Å.

The AIM analysis demonstrates the presence of bond critical points (BCPs) (3, −1) for chalcogen bonding S···Cl and S···N in **KR1**, **KR7**, **TR1**, and **TR7** both in the solid state and in $CHCl_3$ solution (Table S3). The geometry optimization for all these species in a $CHCl_3$ solution leads to elongation of the S···Cl and S···N contacts (by 0.045 Å for **KR1**, 0.038 Å for **KR7**, 0.058 Å for **TR1**, and 0.020 Å for **TR7**) compared to their solid state geometries. The low magnitude of the electron density (0.015−0.026 hartree), positive values of the Laplacian (0.051−0.080 hartree), and close to zero energy density (0.001−0.002 hartree) in these BCPs are typical for noncovalent interactions.

DOI: 10.1021/jacs.6b09133
J. Am. Chem. Soc. 2016, 138, 14129−14137

Table 2. Energies of CBs Defined by Espinosa et al.[37] and Vener et al.[38] Approaches and Relative Stabilities of Isomers

	E_{cb}, kcal/mol		$\Delta G(CHCl_3)$, kcal/mol		ΔE_{cb}, kcal/mol
isomer	solid state	$CHCl_3$ solution	calculated	experimental (based on K_{eq})	$CHCl_3$ solution
KR1	3.1[a]; 3.2[b]	2.8[a]; 3.0[b]	3.2	1.2	1.8−2.0
TR1	6.0[a]; 5.1[b]	5.0[a]; 4.6[b]			
KR7	3.1[a]; 3.2[b]	2.8[a]; 3.0[b]	2.1	0.1	1.6−2.5
TR7	5.3[a]; 4.9[b]	5.3[a]; 4.6[b]			

[a]Ref 37. [b]Ref 38.

We have defined energies for these contacts according to the procedures proposed by Espinosa et al.[37] and Vener et al.[38] (Table S3). The balance between the Lagrangian kinetic energy $G(\mathbf{r})$ and potential energy density $V(\mathbf{r})$ at the bond critical points (3, −1) reveals the nature of these interactions, if the ratio $-G(\mathbf{r})/V(\mathbf{r}) > 1$ is satisfied, than the nature of appropriate interaction is purely noncovalent, in case the $-G(\mathbf{r})/V(\mathbf{r}) < 1$ some covalent component takes place.[39] On the basis of this criterion one can state that the covalent contribution in the chalcogen bonding S···Cl and S···N in all structures under study is absent both in the solid state and in $CHCl_3$. The negligible nonzero or zero values of the Wiberg bond indices for the S···Cl and S···N contacts in the equilibrium structures of **KR1**, **KR7**, **TR1**, and **TR7** in $CHCl_3$ (0.04 for **KR1**, 0.00 for **KR7**, 0.03 for **TR1**, and 0.05 for **TR7**) additionally confirms the electrostatic nature of these noncovalent interactions.

On the basis of the results of AIM analysis (Table S3) it is clear that the S···N contacts in **TR1** and **TR7** (4.9−6.0 kcal/mol in the solid state and 4.6−5.3 kcal/mol in $CHCl_3$) are stronger than the S···Cl contacts in **KR1** and **KR7** (3.1−3.2 kcal/mol in the solid state and 2.8−3.0 kcal/mol in $CHCl_3$), and appropriate interaction energies are typical for CBs.[1b,c,40] We also determined relative stability of these isomers in $CHCl_3$ solution (Table 2, for more details see Table S4, Supporting Information) and in both cases **TR** is more stable than **KR**. In the case of 1,3-thiazole compounds, energy difference for the equilibrium structures of **KR1** and **TR1** is 3.2 kcal/mol in terms of Gibbs free energies, whereas for 1,3,4-thiadiazole species (**KR7** and **TR7**) it is only 2.1 kcal/mol (Table S4). Taking into account systematic overestimation of these thermodynamic parameters[1a,41] (approximately by 2 kcal/mol) and after introducing the corresponding amendment, these results agreeable with the experimental data (Table 2).

The difference in energies of S···N contact in **TR1** and S···Cl contact in **KR1** (1.8−2.0 kcal/mol in $CHCl_3$) correlates well with relative stability of these isomers (ΔG experimental = 1.2 kcal/mol and ΔG calculated = 3.2 kcal/mol, Figure 7). Thus, we assume that in this case the S···N and S···Cl chalcogen bonds make a dominant contribution to the stabilization of isomer **TR1** comparing to **KR1**. For **TR7** and **KR7**, despite the slightly greater gap in energies of S···N and S···Cl contacts (1.6−2.5 kcal/mol in $CHCl_3$), the difference in the relative stability of these isomers is less noticeable (ΔG experimental = 0.1 kcal/mol and ΔG calculated = 2.1 kcal/mol).

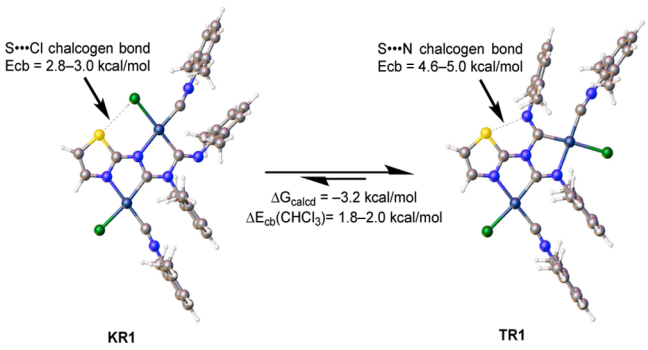

Figure 7. Energy difference of the equilibrium structures of **TR1** and **KR1** and the chalcogen bonds.

We assumed that possible reason for different behavior of **KR**/**TR1** and **KR**/**TR7** is the difference in energies of the Pd−N and C−N bonds. In order to verify this hypothesis, we evaluated the vertical total energies of **KR1**, **KR7**, **TR1**, and **TR7** dissociation (E_v) through the Pd−N, C−N, and S···Cl/S···N contacts (Scheme 3). Calculated E_v values are 243.2 (**KR1**), 242.2 (**KR7**), 247.1 (**TR1**), and 243.3 (**TR7**) kcal/mol, and this is agree well with K_{eq} parameters: in the case of **KR**/**TR1**, the thermodynamically controlled regioisomer **TR1** is noticeably more resistant to decomposition (by 3.9 kcal/mol), whereas for **KR**/**TR7** both regioisomers are prone to decompose similarly (difference in E_v values is only 1.1 kcal/mol). The difference of calculated vertical total energies without the contribution of CB for **KR**/**TR1** is 1.9−2.1 kcal/mol, and the thermodynamically controlled regioisomer **TR1** in such case is still more resistant to decomposition. At the same time, if we consider the calculated vertical total energies without the contribution of CB for **KR**/**TR7** pair, the **KR7** should be more resistant to decomposition than the **TR7** (by 0.8−1.4 kcal/mol), but accounting for the CB contribution dramatically changes the situation, and **TR7** becomes more stable.

Scheme 3. Cleavage of the Pd−N and C−N Bonds, and the S···Cl/S···N Contacts in KR1, KR7, TR1, and TR7

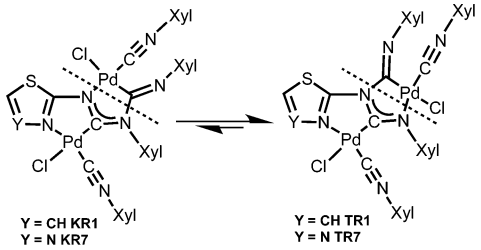

CONCLUSIONS

The reaction between the isocyanide−palladium(II) complex *cis*-$[PdCl_2(CNXyl)_2]$ and two classes of heterocyclic systems—1,3-thiazol-2-amines (**1**−**6**) and 1,3,4-thiadiazol-2-amines (**7**−**9**)—affords binuclear complexes **KR**/**TR1**−**9** as mixtures of kinetically (**KR**) and thermodynamically (**TR**) controlled regioisomers. The structures of all these species featuring two fused 5-membered palladacycles were determined by 1D (^1H, $^{13}C\{^1H\}$) and 2D (^1H,^1H-COSY, ^1H,^1H-NOESY, ^1H,^{13}C-

DOI: 10.1021/jacs.6b09133
J. Am. Chem. Soc. 2016, 138, 14129−14137

HSQC, $^{1}H,^{13}C$-HMBC) NMR in $CDCl_3$ solutions and X-ray diffraction in the solid state (six structures). Remarkable that each pair of the isomers exhibits two different types of chalcogen bonding such as S···Cl (**KRs**) and S···N (**TRs**); the presence of CBs has been proved by combined X-ray crystallographic and DFT study.

In $CDCl_3$ solutions, we observed interconversion of **KRs** and **TRs** giving equilibrium mixtures of both isomers. Results of DFT calculations followed by the topological analysis of the electron density distribution within the formalism of Bader's theory (AIM method) revealed that in $CHCl_3$ solution the relative stability of the regioisomers (ΔG_{exp} = 1.2 kcal/mol; ΔG_{calcd} = 3.2 kcal/mol) is determined by the energy difference between two types of the intramolecular chalcogen bonds, viz. S···Cl in **KRs** (2.8−3.0 kcal/mol) and S···N in **TRs** (4.6−5.3 kcal/mol). In the case of the 1,3,4-thiadiazol-2-amines, the regioisomers are formed in approximately equal amounts and, accordingly, the energy difference between these species is only 0.1 kcal/mol (ΔG_{calcd} = 2.1 kcal/mol). The different behavior of 1,3-thiazol-2-amine and 1,3,4-thiadiazol-2-amine derivatives determined by the different strengths of the Pd−N and C−N bonds. The studied systems provide the first example when the chemical reaction is driven by the energy difference between two types of CB, viz. S···Cl and S···N. Noteworthy that, in principle, CB could also preorganize the reactants in preference of the kinetic regioisomer prior to bond/ring formation, and further studies in this direction are under way in our group.

EXPERIMENTAL SECTION

Materials and Instrumentation. Solvents, $PdCl_2$, heterocycles **1**, **2**, **6**−**9**, and xylyl isocyanide were obtained from commercial sources and used as received, apart from chloroform, which was dried by the distillation over calcium chloride. Complex *cis*-$[PdCl_2(CNXyl)_2]$[42] and heterocycles **3**−**5**[43] were synthesized by the modified literature procedures. C, H, and N elemental analyses were carried out on a Euro EA 3028 HT CHNSO analyzer. Mass-spectra were obtained on a Bruker micrOTOF spectrometer equipped with electrospray ionization (ESI) source, a mixture of MeOH and CH_2Cl_2 was used for samples dissolution. The instrument was operated at a positive ion mode using m/z range of 50−3000. The capillary voltage of the ion source was set at −4500 V and the capillary exit at 50−150 V. The nebulizer gas pressure was 0.4 bar and the drying gas flow 4.0 L/min. The most intensive peak in the isotopic pattern is reported. Infrared spectra were recorded on a PerkinElmer Spectrum BX FT-IR spectrometer (4000−400 cm^{-1}) in KBr pellets for solid samples and in IR cells (KBr, l = 1.05 mm) for chloroform solutions. 1D (^{1}H, $^{13}C\{^{1}H\}$) NMR spectra were acquired on a Bruker Avance 400 spectrometer, while 2D (^{1}H, ^{1}H-COSY, $^{1}H,^{1}H$-NOESY, ^{1}H, ^{13}C-HMQC/HSQC, and $^{1}H,^{13}C$-HMBC) NMR correlation experiments were recorded on a Bruker Avance II+ 500 MHz (UltraShield Magnet) spectrometer. All NMR spectra were acquired in $CDCl_3$ at ambient temperature.

Synthetic Work. A solution of any one of **1**−**9** (0.068 mmol) ((i) in CH_2Cl_2 (3 mL) or (ii) in $CHCl_3$ (5 mL) for generation of mixtures enriched with **KR** or **TR**, correspondingly) was added to solid **PC** (20 mg, 0.045 mmol) placed in a 10 mL round-bottom flask. The reaction mixtures were stirred in air (i) at RT for 24 h (48 h in the case of **6**) giving **KR**/**TR** mixtures enriched with **KR** or (ii) upon reflux for 12 h for the mixtures enriched with **TR**. In all cases, the color of the reaction mixtures gradually turned from pale yellow to intense lemon yellow and solid **PC** was dissolved. The formed solutions were filtered from some insoluble material and evaporated at 20−25 °C to dryness and then the solid residues were washed with Et_2O (three 1 mL portions) and dried in air at RT. The yields, isomeric ratios, and elemental analyses data for the obtained mixtures are given in Table S1.

Pure **KRs** and **TRs** were obtained by dissolution of the isomeric mixtures (Table S1) enriched with **KR** or **TR** (except **TR5** which was obtained from equilibrium mixture), respectively, in acetone (1.5 mL)/CH_2Cl_2 (2 mL) mixture and then these solutions were left to evaporate at 20−25 °C to ca. 1 mL. In case of **KR9**, **TR8**, and **TR9**, one additional recrystallization from acetone/CH_2Cl_2 mixture was performed. The formed crystals of pure isomers were filtered off, washed with Et_2O (three 1 mL portions) and dried in air at 20−25 °C. Pure complexes were obtained as yellow solids and characterized by HRESI^{+}-MS, IR, 1D (^{1}H, $^{13}C\{^{1}H\}$) and 2D ($^{1}H,^{1}H$-COSY, $^{1}H,^{1}H$-NOESY, $^{1}H,^{13}C$-HSQC, $^{1}H,^{13}C$-HMBC) NMR spectroscopies. Our attempts to isolate pure complexes **KR6** and **TR7** failed and these species were characterized only by ^{1}H NMR as a component of certain isomeric mixture.

Characterization. Characterization data, ^{1}H, $^{13}C\{^{1}H\}$ and HMBC NMR spectra are included in Supporting Information.

Equilibrium Measurements for KR1. (i) NMR study. Complex **KR1** (9 mg, 10 μmol) and $CDCl_3$ (0.5 mL) were placed into an NMR tube, which was thermostated at 45 °C. The ^{1}H NMR spectra were acquired every 1−2 days until equilibrium **KR1**/**TR1** had been reached (ca. 13 days) as judged by integral ratios of the Xyl-H^4 peaks. (ii) IR study. Complex **KR1** (5 mg, 5.5 μmol) was dissolved in $CHCl_3$ (0.5 mL) and the solution was placed in an IR cell, which was then placed in thermostat at 45 °C. The IR spectra were measured every 30 min for the first 6 h and then after 6 h gap every 1 h for the next 6 h.

Equilibrium Measurements for Other Complexes. In case of other complexes, the mixtures of both regioisomers (9 mg in every case) and $CDCl_3$ (0.5 mL) were placed into NMR tubes, which were thermostated at 45 °C until the equilibrium was established. The isomeric ratios were determined by NMR integration of the Xyl-H^4 resonances.

X-ray Structure Determinations. Single crystals of **KR1**, **KR7**, **TR8**, and **KR9** were grown from acetone/CH_2Cl_2 mixtures and that of **TR1** and **TR7** from a $Et_2O/CHCl_3$ mixture. The X-ray experiments were conducted on a SuperNova, Dual, Cu at zero, Atlas diffractometer of **KR1**, **TR1** and on a Xcalibur, Eos diffractometer of **KR7**, **TR8**, **TR7**, and **KR9**. The crystals were kept at 100(2) K during data collection. Using Olex2,[44] the structure was solved with the Superflip[45] structure solution program using Charge Flipping (**KR1**, **TR8**) and with the ShelXS[45] using Direct Methods (**TR1**, **KR7**, **TR7**, **KR9**) and all structures were refined with the ShelXL[45] refinement package using Least Squares minimization. The carbon-bound H atoms were placed in calculated positions and were included in the refinement in the "riding" model approximation, with $U_{iso}(H)$ set to $1.5U_{eq}(C)$ and C−H 0.96 Å for the CH_3 groups, with $U_{iso}(H)$ set to $1.2U_{eq}(C)$ and C−H 0.93 Å for the CH groups. Empirical absorption correction was applied in CrysAlisPro[46] program complex using spherical harmonics implemented in SCALE3 ABSPACK scaling algorithm.

Computational Details. The full geometry optimization and single point calculations based on the experimental X-ray geometries (quasi-solid-state approach) have been carried out at DFT level of theory using the M06 functional[47] (this functional was specifically developed to describe weak dispersion forces and noncovalent interactions) with the help of Gaussian-09[48] program package. The calculations were performed using the quasi-relativistic Stuttgart pseudopotentials that described 28 core electrons and the appropriate contracted basis sets[49] for the palladium atoms and the 6-31G* basis sets for other atoms. No symmetry restrictions have been applied during the geometry optimization. The solvent effects were taken into account using the SMD continuum solvation model by Truhlar et al.[50] with $CHCl_3$ as solvent. The Hessian matrix was calculated analytically for the optimized structures in order to prove the location of correct minima (no imaginary frequencies), and to estimate the thermodynamic parameters, the latter being calculated at 25 °C. The topological analysis of the electron density distribution with the help of the atoms in molecules (AIM) method developed by Bader[35] has been performed by using the Multiwfn program (version 3.3.4).[51] The Wiberg bond indices were computed by using the natural bond orbital (NBO) partitioning scheme.[52] The Cartesian atomic coordinates of

DOI: 10.1021/jacs.6b09133
J. Am. Chem. Soc. 2016, 138, 14129−14137

the calculated equilibrium structures in $CHCl_3$ solution are presented in Table S5 (Supporting Information).

■ ASSOCIATED CONTENT

Supporting Information

The Supporting Information is available free of charge on the ACS Publications website at DOI: 10.1021/jacs.6b09133.

Experimental details for the synthesis and characterization of the complexes, NMR spectra, crystallographic and computational information (PDF)
Crystal data (CIF)

■ AUTHOR INFORMATION

Corresponding Authors

*v.boiarskii@spbu.ru
*v.kukushkin@spbu.ru

Notes

The authors declare no competing financial interest.

■ ACKNOWLEDGMENTS

This work was supported by Russian Science Foundation (grant 14-43-00017). Physicochemical studies were performed at the Center for Magnetic Resonance, Center for X-ray Diffraction Studies, Center for Chemical Analysis and Materials Research, and Chemistry Educational Centre (all belong to Saint Petersburg State University).

■ REFERENCES

(1) (a) Bauza, A.; Alkorta, I.; Frontera, A.; Elguero, J. *J. Chem. Theory Comput.* **2013**, *9*, 5201−5210. (b) Wang, W.; Ji, B.; Zhang, Y. *J. Phys. Chem. A* **2009**, *113*, 8132−8135. (c) Bleiholder, C.; Werz, D. B.; Koppel, H.; Gleiter, R. *J. Am. Chem. Soc.* **2006**, *128*, 2666−2674. (d) Bauza, A.; Quinonero, D.; Deya, P. M.; Frontera, A. *CrystEngComm* **2013**, *15*, 3137−3144. (e) Cavallo, G.; Metrangolo, P.; Pilati, T.; Resnati, G.; Terraneo, G. *Cryst. Growth Des.* **2014**, *14*, 2697−2702.

(2) (a) Iwaoka, M.; Isozumi, N. *Molecules* **2012**, *17*, 7266−7283. (b) Iwaoka, M.; Takemoto, S.; Tomoda, S. *J. Am. Chem. Soc.* **2002**, *124*, 10613−10620. (c) Iwaoka, M.; Babe, N. *Phosphorus, Sulfur, Silicon Relat. Elem.* **2015**, *190*, 1257−1264. (d) Lange, A.; Guenther, M.; Buettner, F. M.; Zimmermann, M. O.; Heidrich, J.; Hennig, S.; Zahn, S.; Schall, C.; Sievers-Engler, A.; Ansideri, F.; Koch, P.; Laemmerhofer, M.; Stehle, T.; Laufer, S. A.; Boeckler, F. M. *J. Am. Chem. Soc.* **2015**, *137*, 14640−14652. (e) Fick, R. J.; Kroner, G. M.; Nepal, B.; Magnani, R.; Horowitz, S.; Houtz, R. L.; Scheiner, S.; Trievel, R. C. *ACS Chem. Biol.* **2016**, *11*, 748−754.

(3) (a) Bissantz, C.; Kuhn, B.; Stahl, M. *J. Med. Chem.* **2010**, *53*, 6241−6241. (b) Beno, B. R.; Yeung, K.-S.; Bartberger, M. D.; Pennington, L. D.; Meanwell, N. A. *J. Med. Chem.* **2015**, *58*, 4383−4438. (c) Reid, R. C.; Yau, M.-K.; Singh, R.; Lim, J.; Fairlie, D. P. *J. Am. Chem. Soc.* **2014**, *136*, 11914−11917. (d) Le, H. V.; Hawker, D. D.; Wu, R.; Doud, E.; Widom, J.; Sanishvili, R.; Liu, D.; Kelleher, N. L.; Silverman, R. B. *J. Am. Chem. Soc.* **2015**, *137*, 4525−4533. (e) Meanwell, N. A. *J. Med. Chem.* **2011**, *54*, 2529−2591. (f) Nagao, Y.; Hirata, T.; Goto, S.; Sano, S.; Kakehi, A.; Iizuka, K.; Shiro, M. *J. Am. Chem. Soc.* **1998**, *120*, 3104−3110.

(4) (a) Jackson, N. E.; Savoie, B. M.; Kohlstedt, K. L.; de la Cruz, M. O.; Schatz, G. C.; Chen, L. X.; Ratner, M. A. *J. Am. Chem. Soc.* **2013**, *135*, 10475−10483. (b) Tian, Y.-H.; Kertesz, M. *Macromolecules* **2009**, *42*, 6123−6127. (c) Yasuda, T.; Sakai, Y.; Aramaki, S.; Yamamoto, T. *Chem. Mater.* **2005**, *17*, 6060−6068. (d) Karikomi, M.; Kitamura, C.; Tanaka, S.; Yamashita, Y. *J. Am. Chem. Soc.* **1995**, *117*, 6791−6792. (e) Ozen, A. S.; Atilgan, C.; Sonmez, G. *J. Phys. Chem. C* **2007**, *111*, 16362−16371.

(5) (a) Suresh, K.; Minkov, V. S.; Namila, K. K.; Derevyannikova, E.; Losev, E.; Nangia, A.; Boldyreva, E. V. *Cryst. Growth Des.* **2015**, *15*, 3498−3510. (b) Mali, S. M.; Schneider, T. F.; Bandyopadhyay, A.; Jadhav, S. V.; Werz, D. B.; Gopi, H. N. *Cryst. Growth Des.* **2012**, *12*, 5643−5648.

(6) (a) Cozzolino, A. F.; Vargas-Baca, I.; Mansour, S.; Mahmoudkhani, A. H. *J. Am. Chem. Soc.* **2005**, *127*, 3184−3190. (b) Cozzolino, A. F.; Elder, P. J. W.; Lee, L. M.; Vargas-Baca, I. *Can. J. Chem.* **2013**, *91*, 338−347. (c) Gleiter, R.; Werz, D. B.; Rausch, B. J. *Chem. - Eur. J.* **2003**, *9*, 2676−2683. (d) Werz, D. B.; Gleiter, R.; Rominger, F. *J. Am. Chem. Soc.* **2002**, *124*, 10638−10639. (e) Werz, D. B.; Staeb, T. H.; Benisch, C.; Rausch, B. J.; Rominger, F.; Gleiter, R. *Org. Lett.* **2002**, *4*, 339−342. (f) Cozzolino, A. F.; Elder, P. J. W.; Vargas-Baca, I. *Coord. Chem. Rev.* **2011**, *255*, 1426−1438. (g) Yasuda, T.; Shimizu, T.; Liu, F.; Ungar, G.; Kato, T. *J. Am. Chem. Soc.* **2011**, *133*, 13437−13444.

(7) Burling, F. T.; Goldstein, B. M. *J. Am. Chem. Soc.* **1992**, *114*, 2313−2320.

(8) (a) Chivers, T.; Laitinen, R. S. *Chem. Soc. Rev.* **2015**, *44*, 1725−1739. (b) Garrett, G. E.; Carrera, E. I.; Seferos, D. S.; Taylor, M. S. *Chem. Commun.* **2016**, *52*, 9881−9884. (c) Garrett, G. E.; Gibson, G. L.; Straus, R. N.; Seferos, D. S.; Taylor, M. S. *J. Am. Chem. Soc.* **2015**, *137*, 4126−4133. (d) Ho, P. C.; Szydlowski, P.; Sinclair, J.; Elder, P. J. W.; Kübel, J.; Gendy, C.; Lee, L. M.; Jenkins, H.; Britten, J. F.; Morim, D. R.; Vargas-Baca, I. *Nat. Commun.* **2016**, *7*, 11299. (e) Si, M. K.; Ganguly, B. *New J. Chem.* **2016**, DOI: 10.1039/C6NJ01707J.

(9) (a) Bai, M.; Thomas, S. P.; Kottokkaran, R.; Nayak, S. K.; Ramamurthy, P. C.; Row, T. N. G. *Cryst. Growth Des.* **2014**, *14*, 459−466. (b) Wang, X.-Y.; Jiang, W.; Chen, T.; Yan, H.-J.; Wang, Z.-H.; Wan, L.-J.; Wang, D. *Chem. Commun.* **2013**, *49*, 1829−1831. (c) Xiao, Q.; Sakurai, T.; Fukino, T.; Akaike, K.; Honsho, Y.; Saeki, A.; Seki, S.; Kato, K.; Takata, M.; Aida, T. *J. Am. Chem. Soc.* **2013**, *135*, 18268−18271.

(10) (a) Khan, I.; Panini, P.; Khan, S. U.-D.; Rana, U. A.; Andleeb, H.; Chopra, D.; Hameed, S.; Simpson, J. *Cryst. Growth Des.* **2016**, *16*, 1371−1386. (b) Amelichev, S. A.; Konstantinova, L. S.; Lyssenko, K. A.; Rakitin, O. A.; Rees, C. W. *Org. Biomol. Chem.* **2005**, *3*, 3496−350. (c) Konstantinova, L. S.; Rakitin, O. A.; Souvorova, L. I.; Rees, C. W.; White, A. J. P.; Williams, D. J.; Torroba, T. *Chem. Commun.* **1999**, 73−74. (d) Iyoda, M.; Suzuki, H.; Sasaki, S.; Yoshino, H.; Kikuchi, K.; Saito, K.; Ikemoto, I.; Matsuyama, H.; Mori, T. *J. Mater. Chem.* **1996**, *6*, 501−503. (e) Raghunandan, R.; Rawal, R. K.; Katti, S. B.; Maulik, P. R. *Acta Crystallogr., Sect. E: Struct. Rep. Online* **2006**, *62*, 5349−5351. (f) Leitch, A. A.; Yu, X.; Winter, S. M.; Secco, R. A.; Dube, P. A.; Oakley, R. T. *J. Am. Chem. Soc.* **2009**, *131*, 7112−7125. (g) Benz, S.; Macchione, M.; Verolet, Q.; Mareda, J.; Sakai, N.; Matile, S. *J. Am. Chem. Soc.* **2016**, *38*, 9093−9096.

(11) (a) Tlahuext, H.; Reyes-Martinez, R.; Vargas-Pineda, G.; Lopez-Cardoso, M.; Hoepfl, H. *J. Organomet. Chem.* **2011**, *696*, 693−701. (b) Yandanova, E. S.; Ivanov, D. M.; Kuznetsov, M. L.; Starikov, A. G.; Starova, G. L.; Kukushkin, V. Y. *Cryst. Growth Des.* **2016**, *16*, 2979−2987. (c) Calderazzo, F.; D'Attoma, M.; Marchetti, F.; Pampaloni, G.; Troyanov, S. I. *J. Chem. Soc., Dalton Trans.* **1999**, 2275−2277. (d) Eriksen, K.; Hauge, S.; Maroy, K. *Phosphorus, Sulfur, Silicon Relat. Elem.* **2001**, *174*, 209−221. (e) Antsyshkina, A. S.; Sadikov, G. G.; Makhaev, V. D.; Shilov, G. V. *Russ. J. Inorg. Chem.* **2012**, *57*, 927−931. (f) Singh, G.; Singh, A. K.; Drake, J. E.; Hursthouse, M. B.; Light, M. E. *Polyhedron* **2006**, *25*, 3481−3487. (g) Dai, J.; Munakata, M.; Bian, G. Q.; Xu, Q. F.; Kuroda-Sowa, T.; Maekawa, M. *Polyhedron* **1998**, *17*, 2267−2270. (h) Virovets, A. V.; Volkov, O. V. *J. Struct. Chem.* **2000**, *41*, 713−716.

(12) (a) Thomas, S. P.; Veccham, S. P. K. P.; Farrugia, L. J.; Row, T. N. G. *Cryst. Growth Des.* **2015**, *15*, 2110−2118. (b) Rethore, C.; Madalan, A.; Fourmigue, M.; Canadell, E.; Lopes, E.; Almeida, M.; Clerac, R.; Avarvari, N. *New J. Chem.* **2007**, *31*, 1468−1483.

(13) Iwaoka, M.; Isozumi, N. *Biophysics (Biophys. Soc. Jpn.)* **2006**, *2*, 23−34.

(14) (a) Fukata, Y.; Asano, K.; Matsubara, S. *J. Am. Chem. Soc.* **2015**, *137*, 5320−5323. (b) West, T. H.; Daniels, D. S. B.; Slawin, A. M. Z.;

DOI: 10.1021/jacs.6b09133
J. Am. Chem. Soc. 2016, 138, 14129−14137

Smith, A. D. *J. Am. Chem. Soc.* **2014**, *136*, 4476−4479. (c) Smith, S. R.; Douglas, J.; Prevet, H.; Shapland, P.; Slawin, A. M. Z.; Smith, A. D. *J. Org. Chem.* **2014**, *79*, 1626−1639. (d) Robinson, E. R. T.; Fallan, C.; Simal, C.; Slawin, A. M. Z.; Smith, A. D. *Chem. Sci.* **2013**, *4*, 2193−2200.
(15) Nagao, Y.; Miyamoto, S.; Miyamoto, M.; Takeshige, H.; Hayashi, K.; Sano, S.; Shiro, M.; Yamaguchi, K.; Sei, Y. *J. Am. Chem. Soc.* **2006**, *128*, 9722−9729.
(16) Chandrasekhar, V.; Chivers, T.; Ellis, L.; Krouse, I.; Parvez, M.; Vargas-Baca, I. *Can. J. Chem.* **1997**, *75*, 1188−1194.
(17) Fukumoto, S.; Nakashima, T.; Kawai, T. *Angew. Chem., Int. Ed.* **2011**, *50*, 1565−1568.
(18) (a) Akiba, K.; Arai, S.; Tsuchiya, T.; Yamamoto, Y.; Iwasaki, F. *Angew. Chem., Int. Ed. Engl.* **1979**, *18*, 166−167. (b) Akiba, K.; Kobayashi, T.; Arai, S. *J. Am. Chem. Soc.* **1979**, *101*, 5857−5858. (c) Akiba, K. Y.; Kashiwagi, K.; Ohyama, Y.; Yamamoto, Y.; Ohkata, K. *J. Am. Chem. Soc.* **1985**, *107*, 2721−2730.
(19) Sawwan, N.; Brzostowska, E. M.; Greer, A. *J. Org. Chem.* **2005**, *70*, 6968−6971.
(20) Cox, P. A.; Leach, A. G.; Campbell, A. D.; Lloyd-Jones, G. C. *J. Am. Chem. Soc.* **2016**, *138*, 9145−9157.
(21) Ruff, F.; Kapovits, I.; Rabai, J.; Kucsman, A. *Tetrahedron* **1978**, *34*, 2767−2773.
(22) Tskhovrebov, A.; Luzyanin, K.; Dolgushin, F.; Guedes da Silva, M. F. C.; Pombeiro, A.; Kukushkin, V. *Organometallics* **2011**, *30*, 3362−3370.
(23) Forlani, L.; Demaria, P.; Fini, A. *J. Chem. Soc., Perkin Trans. 2* **1980**, 1156−1158.
(24) Perrin, D. D.; Dempsey, B.; Serjeant, E. P. *pKa Prediction for Organic Acids and Bases*; Chapman and Hall: London, 1981.
(25) (a) Martinez-Martinez, A.; Chicote, M.; Bautista, D.; Vicente, J. *Organometallics* **2012**, *31*, 3711−3719. (b) Wanniarachchi, Y.; Slaughter, L. *Chem. Commun.* **2007**, 3294−3296. (c) Luzyanin, K.; Pombeiro, A.; Haukka, M.; Kukushkin, V. *Organometallics* **2008**, *27*, 5379−5389. (d) Kinzhalov, M.; Boyarskiy, V.; Luzyanin, K.; Dolgushin, F.; Kukushkin, V. *Dalton Trans.* **2013**, *42*, 10394−10397. (e) Kinzhalov, M.; Luzyanin, K.; Boyarskiy, V.; Haukka, M.; Kukushkin, V. *Organometallics* **2013**, *32*, 5212−5223. (f) Valishina, E.; Guedes da Silva, M. F. C.; Kinzhalov, M.; Timofeeva, S.; Buslaeva, T.; Haukka, M.; Pombeiro, A.; Boyarskiy, V.; Kukushkin, V.; Luzyanin, K. *J. Mol. Catal. A: Chem.* **2014**, *395*, 162−171. (g) Timofeeva, S.; Kinzhalov, M.; Valishina, E.; Luzyanin, K.; Boyarskiy, V.; Buslaeva, T.; Haukka, M.; Kukushkin, V. *J. Catal.* **2015**, *329*, 449−456. (h) Kinzhalov, M. A.; Timofeeva, S. A.; Luzyanin, K. V.; Boyarskiy, V. P.; Yakimanskiy, A. A.; Haukka, M.; Kukushkin, V. Y. *Organometallics* **2016**, *35*, 218−228.
(26) Drouin, M.; Perreault, D.; Harvey, P.; Michel, A. *Acta Crystallogr., Sect. C: Cryst. Struct. Commun.* **1991**, *47*, 752−754.
(27) Kinzhalov, M. A.; Luzyanin, K. V.; Boyarskaya, I. A.; Starova, G. L.; Boyarskiy, V. P. *J. Mol. Struct.* **2014**, *1068*, 222−227.
(28) Allen, F.; Kennard, O.; Watson, D.; Brammer, L.; Orpen, A.; Taylor, R. *J. Chem. Soc., Perkin Trans. 2* **1987**, S1−S19.
(29) Rowland, R.; Taylor, R. *J. Phys. Chem.* **1996**, *100*, 7384−7391.
(30) Bondi, A. *J. Phys. Chem.* **1964**, *68*, 441−451.
(31) Rosenfield, R. E.; Parthasarathy, R.; Dunitz, J. D. *J. Am. Chem. Soc.* **1977**, *99*, 4860−4862.
(32) Butler, A. R.; Glidewell, C.; Liles, D. C. *Acta Crystallogr., Sect. B: Struct. Crystallogr. Cryst. Chem.* **1978**, *34*, 2570−2574.
(33) (a) Moncada, A.; Manne, S.; Tanski, J.; Slaughter, L. *Organometallics* **2006**, *25*, 491−505. (b) Kitano, Y.; Hori, T. *Acta Crystallogr., Sect. B: Struct. Crystallogr. Cryst. Chem.* **1981**, *37*, 1919−1921. (c) Perreault, D.; Drouin, M.; Michel, A.; Harvey, P. *Inorg. Chem.* **1993**, *32*, 1903−1912. (d) Domiano, P.; Musatti, A.; Nardelli, M.; Predieri, G. *J. Chem. Soc., Dalton Trans.* **1975**, 2165−2168.
(34) Wanniarachchi, Y.; Slaughter, L. *Organometallics* **2008**, *27*, 1055−1062.
(35) Bader, R. F. W. *Chem. Rev.* **1991**, *91*, 893−928.
(36) (a) Ivanov, D. M.; Novikov, A. S.; Ananyev, I. V.; Kirina, Y. V.; Kukushkin, V. Y. *Chem. Commun.* **2016**, *52*, 5565−5568. (b) Ding, X.; Tuikka, M. J.; Hirva, P.; Kukushkin, V. Y.; Novikov, A. S.; Haukka, M. *CrystEngComm* **2016**, *18*, 1987−1995. (c) Mikhaylov, V. N.; Sorokoumov, V. N.; Korvinson, K. A.; Novikov, A. S.; Balova, I. A. *Organometallics* **2016**, *35*, 1684−1697. (d) Ivanov, D. M.; Novikov, A. S.; Starova, G. L.; Haukka, M.; Kukushkin, V. Y. *CrystEngComm* **2016**, *18*, 5278−5286. (e) Serebryanskaya, T. V.; Novikov, A. S.; Gushchin, P. V.; Haukka, M.; Asfin, R. E.; Tolstoy, P. M.; Kukushkin, V. Y. *Phys. Chem. Chem. Phys.* **2016**, *18*, 14104−14112. (f) Novikov, A. S.; Kuznetsov, M. L.; Pombeiro, A. J. L. *Chem. - Eur. J.* **2013**, *19*, 2874−2888.
(37) Espinosa, E.; Molins, E.; Lecomte, C. *Chem. Phys. Lett.* **1998**, *285*, 170−173.
(38) Vener, M. V.; Egorova, A. N.; Churakov, A. V.; Tsirelson, V. G. *J. Comput. Chem.* **2012**, *33*, 2303−2309.
(39) Espinosa, E.; Alkorta, I.; Elguero, J.; Molins, E. *J. Chem. Phys.* **2002**, *117*, 5529−5542.
(40) (a) Bleiholder, C.; Gleiter, R.; Werz, D. B.; Koppel, H. *Inorg. Chem.* **2007**, *46*, 2249−2260. (b) Alikhani, E.; Fuster, F.; Madebene, B.; Grabowski, S. J. *Phys. Chem. Chem. Phys.* **2014**, *16*, 2430−2442. (c) Adhikari, U.; Scheiner, S. *J. Phys. Chem. A* **2014**, *118*, 3183−3192. (d) Esrafili, M. D.; Mohammadian-Sabet, F. *Chem. Phys. Lett.* **2015**, *634*, 210−215. (e) Nepal, B.; Scheiner, S. *Chem. Phys.* **2015**, *456*, 34−40. (f) Nziko, V. d. P. N.; Scheiner, S. *J. Phys. Chem. A* **2014**, *118*, 10849−10856. (g) Azofra, L. M.; Alkorta, I.; Scheiner, S. *Theor. Chem. Acc.* **2014**, *133*, 133. (h) Murray, J. S.; Lane, P.; Clark, T.; Politzer, P. *J. Mol. Model.* **2007**, *13*, 1033−1038.
(41) (a) Marianski, M.; Asensio, A.; Dannenberg, J. J. *J. Chem. Phys.* **2012**, *137*, 044109. (b) Sumimoto, M.; Kawashima, Y.; Yokogawa, D.; Hori, K.; Fujumoto, H. *Int. J. Quantum Chem.* **2013**, *113*, 272−276.
(42) Crociani, B.; Boschi, T.; Belluco, U. *Inorg. Chem.* **1970**, *9*, 2021−2025.
(43) English, J. P.; Clark, J. H.; Clapp, J. W.; Seeger, D.; Ebel, R. H. *J. Am. Chem. Soc.* **1946**, *68*, 453−458.
(44) Dolomanov, O.; Bourhis, L.; Gildea, R.; Howard, J.; Puschmann, H. *J. Appl. Crystallogr.* **2009**, *42*, 339−341.
(45) Sheldrick, G. *Acta Crystallogr., Sect. A: Found. Crystallogr.* **2008**, *64*, 112−122.
(46) *CrysAlisPro*, 1.171.36.20; Agilent Technologies: 2012.
(47) Zhao, Y.; Truhlar, D. G. *Theor. Chem. Acc.* **2008**, *120*, 215−241.
(48) Frisch, M. J.; Trucks, G. W.; Schlegel, H. B.; Scuseria, G. E.; Robb, M. A.; Cheeseman, J. R.; Scalmani, G.; Barone, V.; Mennucci, B.; Petersson, G. A.; Nakatsuji, H.; Caricato, M.; Li, X.; Hratchian, H. P.; Izmaylov, A. F.; Bloino, J.; Zheng, G.; Sonnenberg, J. L.; Hada, M.; Ehara, M.; Toyota, K.; Fukuda, R.; Hasegawa, J.; Ishida, M.; Nakajima, T.; Honda, Y.; Kitao, O.; Nakai, H.; Vreven, T.; Montgomery, J. A.; Peralta, J. E.; Ogliaro, F.; Bearpark, M.; Heyd, J. J.; Brothers, E.; Kudin, K. N.; Staroverov, V. N.; Kobayashi, R.; Normand, J.; Raghavachari, K.; Rendell, A.; Burant, J. C.; Iyengar, S. S.; Tomasi, J.; Cossi, M.; Rega, N.; Millam, J. M.; Klene, M.; Knox, J. E.; Cross, J. B.; Bakken, V.; Adamo, C.; Jaramillo, J.; Gomperts, R.; Stratmann, R. E.; Yazyev, O.; Austin, A. J.; Cammi, R.; Pomelli, C.; Ochterski, J. W.; Martin, R. L.; Morokuma, K.; Zakrzewski, V. G.; Voth, G. A.; Salvador, P.; Dannenberg, J. J.; Dapprich, S.; Daniels, A. D.; Farkas, J.; Foresman, B.; Ortiz, J. V.; Cioslowski, J.; Fox, D. J. *Gaussian 09*, Revision C.01; Gaussian, Inc.: Wallingford, CT, 2010.
(49) Andrae, D.; Haussermann, U.; Dolg, M.; Stoll, H.; Preuss, H. *Theor. Chim. Acta* **1990**, *77*, 123−141.
(50) Marenich, A. V.; Cramer, C. J.; Truhlar, D. G. *J. Phys. Chem. B* **2009**, *113*, 6378−6396.
(51) Lu, T.; Chen, F. W. *J. Comput. Chem.* **2012**, *33*, 580−592.
(52) Glendening, E. D.; Landis, C. R.; Weinhold, F. *Wiley Interdiscip. Rev.: Comput. Mol. Sci.* **2012**, *2*, 1−42.

DOI: 10.1021/jacs.6b09133
J. Am. Chem. Soc. 2016, 138, 14129−14137